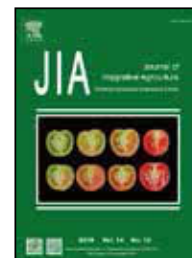




Available online at [www.sciencedirect.com](http://www.sciencedirect.com)

ScienceDirect



RESEARCH ARTICLE

## Water consumption in summer maize and winter wheat cropping system based on SEBAL model in Huang-Huai-Hai Plain, China



CrossMark

YANG Jian-ying<sup>1</sup>, MEI Xu-rong<sup>2</sup>, HUO Zhi-guo<sup>1</sup>, YAN Chang-rong<sup>2</sup>, JU Hui<sup>3</sup>, ZHAO Feng-hua<sup>4</sup>, LIU Qin<sup>2</sup>

<sup>1</sup> Chinese Academy of Meteorological Sciences, Beijing 100081, P.R.China

<sup>2</sup> Key Laboratory of Dryland Agriculture, Ministry of Agriculture/Institute of Environment and Sustainable Development in Agriculture, Chinese Academy of Agricultural Sciences, Beijing 100081, P.R.China

<sup>3</sup> Key Laboratory of Agricultural Environment, Ministry of Agriculture/Institute of Environment and Sustainable Development in Agriculture, Chinese Academy of Agricultural Sciences, Beijing 100081, P.R.China

<sup>4</sup> Key Laboratory of Ecosystem Network Observation and Modeling, Institute of Geographic Sciences and Natural Resources Research, Chinese Academy of Sciences, Beijing 100101, P.R.China

### Abstract

Crop consumptive water use is recognized as a key element to understand regional water management performance. This study documents an attempt to apply a regional evapotranspiration model (SEBAL) and crop information for assessment of regional crop (summer maize and winter wheat) actual evapotranspiration ( $ET_a$ ) in Huang-Huai-Hai (3H) Plain, China. The average seasonal  $ET_a$  of summer maize and winter wheat were 354.8 and 521.5 mm respectively in 3H Plain. A high- $ET_a$  belt of summer maize occurs in piedmont plain, while a low  $ET_a$  area was found in the hill-irrigable land and dry land area. For winter wheat, a high- $ET_a$  area was located in the middle part of 3H Plain, including low plain-hydroponia irrigable land and dry land, hill-irrigable land and dry land, and basin-irrigable land and dry land. Spatial analysis demonstrated a linear relationship between crop  $ET_a$ , normalized difference vegetation index (NDVI), and the land surface temperature (LST). A stronger relationship between  $ET_a$  and NDVI was found in the metaphase and last phase than other crop growing phase, as indicated by higher correlation coefficient values. Additionally, higher correlation coefficients were detected between  $ET_a$  and LST than that between  $ET_a$  and NDVI, and this significant relationship ran through the entire crop growing season.  $ET_a$  in the summer maize growing season showed a significant relationship with longitude, while  $ET_a$  in the winter wheat growing season showed a significant relationship with latitude. The results of this study will serve as baseline information for water resources management of 3H Plain.

**Keywords:**  $ET_a$ , winter wheat, summer maize, SEBAL, crop information, Huang-Huai-Hai Plain

### 1. Introduction

Agriculture is the largest water-consuming sector (FAO 1994; Rosegrant *et al.* 2002) and irrigated agriculture has been expanding rapidly in many developing countries in recent decades, nearly doubling between 1962 and 1998 (Carruthers *et al.* 1997; Ali and Talukder 2008). During com-

Received 5 August, 2014 Accepted 5 January, 2015  
YANG Jian-ying, E-mail: yangjy@cams.cma.gov.cn;  
Correspondence LIU Qin, Tel/Fax: +86-10-82106018,  
E-mail: liuqin02@caas.cn

© 2015, CAAS. All rights reserved. Published by Elsevier Ltd.  
doi: 10.1016/S2095-3119(14)60951-5

ing decades, water may become the most strategic resource, especially for agricultural production in arid and semi-arid regions of the world (Brewster *et al.* 2006), which could threaten the sustainability of world agriculture. Accordingly, understanding the quantity of agricultural water consumption is a high priority in areas in which water is currently scarce and over-exploited (Perry 2011). Evapotranspiration (ET) is a useful indicator of crop water consumption; therefore, accurate estimation of regional ET is essential to achieve large scale water resources management (Rwasoka *et al.* 2011). Current estimates of actual evapotranspiration in China are mainly based on plot-scale experiments (Zhang *et al.* 1999; Chen *et al.* 2002; Sun *et al.* 2003; Jiang and Zhang 2004), from the product of soil moisture and potential ET. However, such estimates are only useful for a specific area, and cannot be expanded to large-scale areas. The level of water consumption differs significantly across regions, farming systems, canal command areas, and farms (Molden *et al.* 2003). These differences come from many factors, including the source of irrigation water, farm management practices, the timing and efficiency of irrigation water in irrigated regions, and conservation tillage technologies, rainwater harvesting and cropping patterns in rainfed areas (Cai and Sharma 2010).

Development of remote sensing technology has made it possible to estimate land surface evapotranspiration at the regional or basin scale. Numerous remote sensing methods for modeling crop actual evapotranspiration ( $ET_a$ ) have been improved (De Oliveira *et al.* 2009; Teixeira *et al.* 2009; Teixeira and Bassoi 2009; Jia *et al.* 2012). Bastiaanssen *et al.* (1998) were the first to use remote sensing data to estimate evapotranspiration in the Bhakra command area, India. And then, several studies demonstrated the strengths of remote sensing in estimating crop evapotranspiration (Courault *et al.* 2005; Allen *et al.* 2007). Accurate estimation of agricultural water consumption is based on two inputs, the model precision, which has been calibrated and validated by many studies, and the ground truth information, including crop dominance maps, phenological characteristics, and agriculture productivity. However, ground truth information is often scarce and difficult to obtain.

Huang-Huai-Hai (3H) Plain is the major crop producing region in China, with 3.5 million ha of highly intensive arable land, accounting for 19% of the country's crop production area. The recognized major limiting factor to crop production in the region is water shortage, which is expected to be exacerbated by increasing food demand in the region (Chen *et al.* 2005). Over exploitation of groundwater resources has resulted in water-table decrease at a rate of 1 m yr<sup>-1</sup> and severe groundwater depression in the past 20 years (Jia and Liu 2002; Wang *et al.* 2009). Moreover, climatic changes have intensified with an average decrease in rainfall

of 2.92 mm yr<sup>-1</sup> (Liu *et al.* 2010). Thus, available agricultural water resources have become the most important factor influencing crop production in 3H Plain, with the regional water scarcity situation becoming aggravated each year. Considering the spatial variation, accurately identification and region-wide water accounting are necessary in 3H Plain, to enable reasonable allocation of the limited available agricultural water resources.

In recent years, Li *et al.* (2008) estimated the  $ET_a$  for winter wheat using the SEBAL (surface energy balance algorithm for land) model and NOAA (National Oceanic and Atmospheric Administration) data for Hebei Province in the North China Plain (NCP). Yang *et al.* (2013) analyzed the spatial and temporal variation of crop evapotranspiration ( $ET_c$ ) and evapotranspiration of applied water ( $ET_{aw}$ ) of summer maize during the growing season from 1960 to 2009 in the 3H farming region using the simulation of evapotranspiration of applied water (SIMETAW) model. However, observed phenological data was not considered in these investigations, and specific water consumption of winter wheat and summer maize has not yet been determined for larger areas in 3H Plain. In this research, an approach to estimate the actual evapotranspiration for summer maize and winter wheat respectively based on the MODIS (moderate-resolution imaging spectroradiometer) data and SEBAL model is proposed and applied in 347 counties of the 3H Plain in China, which is a farming region providing about 61 and 31% of the nation's wheat and maize production (Wang *et al.* 2009; Ma *et al.* 2013). The purpose of this study was: (1) to quantify actual evapotranspiration for winter wheat and summer maize; (2) to determine the spatial pattern of the  $ET_a$  of the two crops grown in 3H Plain; and (3) to identify the relationship between crop  $ET_a$  and land surface parameters and geographic parameters. The findings from this research will provide useful information for agricultural water management practices for 3H Plain, China.

## 2. Results

### 2.1. Crop $ET_a$

The  $ET_a$  of summer maize and winter wheat were calculated based on the crop dominant maps and phenological data. The  $ET_a$  map and histogram distribution, as well as its basic information are described in Table 1 and Fig. 1. The seasonal average  $ET_a$  of summer maize was 354.8 mm at 3H Plain, with a minimum value of 239.4 mm and a maximum value of 552.3 mm. As shown in Fig. 1-A, a high-ET belt occurs in the piedmont plain, from Beijing, Tianjin to the southern part of Hebei Province. The low  $ET_a$  area of summer maize was mainly found in the hill-irrigable land and dry land (Zone 4) area in Shandong Province. The total winter wheat  $ET_a$  was

**Table 1** Actual evapotranspiration ( $ET_a$ ) of summer maize and winter wheat in the study area

	Average $ET_a$ (mm)	Maximum $ET_a$ (mm)	Minimum $ET_a$ (mm)
Summer maize	354.8	552.3	239.4
Winter wheat	521.5	729.2	131.6

comparatively higher than the summer maize  $ET_a$ , with an average value of 521.5 mm. The maximum  $ET_a$  for winter wheat was 729.2 mm, which was found in the middle part of 3H Plain, while the minimum value was 131.6 mm in the southeast part of Hebei Province. An  $ET_a$  between 500 and 600 mm was detected in more than 40% of the winter wheat cover area, although significant variations in this value were observed (Fig. 2). Difference from the summer maize  $ET_a$  map, higher  $ET_a$  area was mainly observed in the middle part of 3H Plain, including low plain-hydroponia irrigable land and dry land (Zone 3), hill-irrigable land and dry land (Zone 4), and basin-irrigable land and dry land (Zone 5). Overall, the  $ET_a$  between summer maize and winter wheat displayed different spatial distributions among levels.

**2.2. Correlation among  $ET_a$ , NDVI, and land surface temperature**

Investigation of the relationship between crop  $ET_a$  and the normalized difference vegetation index (NDVI) and the land surface temperature (LST) are helpful in understanding the effects of NDVI and LST changes on  $ET_a$  for winter wheat and summer maize in time series. Correlation coefficient analysis of the  $ET_a$  values of the two crops with NDVI and then LST for different Julian days. The  $ET_a$  value, NDVI and LST of the two crops were extracted from each raster in space. The relationships between  $ET_a$  and NDVI and  $ET_a$  and LST in the summer maize and winter wheat growing

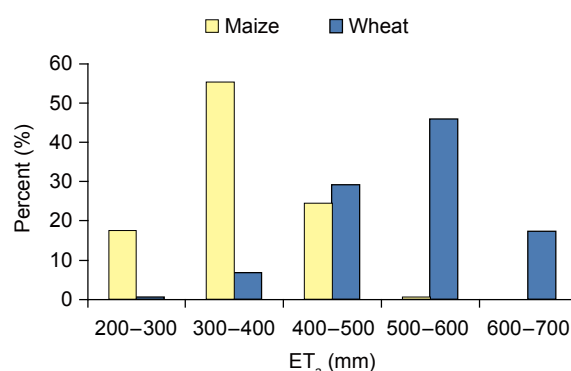


**Fig. 1** Distribution of actual evapotranspiration ( $ET_a$ ) in summer maize season and winter wheat in Huang-Huai-Hai (3H) Plain.

seasons are shown in Tables 2 and 3, respectively.

NDVI is one of the most important parameters to the estimation of actual ET in many models. The results of this study showed that  $ET_a$  increased with NDVI. The linear relationship between  $ET_a$  and NDVI was consistent with results of a previous study by Wang *et al.* (2012). NDVI in the metaphase and last phase was more closed related to  $ET_a$  during the crop growing season, indicated by a higher positive correlation coefficient value. The positive relationship between  $ET_a$  and NDVI in the winter wheat growing season was stronger than in the summer maize growing season in the metaphase and last phase, as indicated by

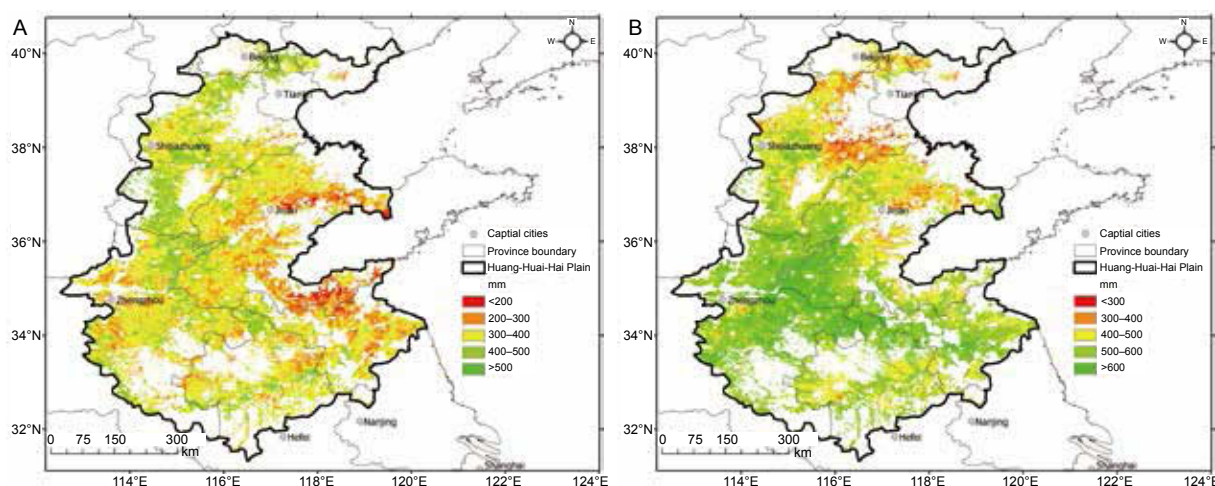


**Fig. 2** Spatial pattern of  $ET_a$  in summer maize-winter wheat rotation in 3H Plain. A, spatial pattern of  $ET_a$  in the summer maize growing season. B, spatial pattern of  $ET_a$  in the winter wheat growing season.

a correlation coefficient value of  $ET_a$  during the summer maize growing season of  $\leq 0.4$ , but as high as 0.6 in the winter wheat growing season. This relationship appears to be stronger in piedmont plain-irrigable land (Zone 2), where the correlation coefficient values reached 0.67. The NDVI index increased strongly in the metaphase and last phase, when crop activities intensified. These changes were expressed as a lower impedance of evapotranspiration and increased latent heat flux in each pixel. This crop physiological reaction may have led to  $ET_a$  increase. These changes were more obvious in flat interior regions, such as piedmont plain-irrigable land, than in basins or hills. The relationship between  $ET_a$  and NDVI was greater during winter and spring, because there was less precipitation participating in the space hydrological cycle.

As described above, a higher value of correlation coefficient was detected between  $ET_a$  and LST than between  $ET_a$  and NDVI, indicating a stronger relationship. The significant relationship between  $ET_a$  and LST ran through the entire crop growing season. Additionally, the correlation between  $ET_a$  and LST was negative, indicating that an increased LST may lead to a decreased  $ET_a$ . In the later portion of the winter wheat growing season in Zone 2 (piedmont plain-irrigable

land), the correlation coefficient value was higher ( $R > 0.7$ ). Temperature is an important factor which is associated with stomatal conductance and transpiration (Yang et al. 2012). For maize, the effect of growth temperature on transpiration was obvious when maize was grown at low temperature (22/18°C) and measured at higher temperature (30°C). The 3H Plain is acknowledged as a water-stress area that primarily receives rainfall during summer. As results, serious drought always occurs in winter and spring, which may impact transpiration and canopy temperature. When crops are subjected to water stress, they close their leaf stomata, which reduces evapotranspiration, leading to increased crop canopy temperature.

### 2.3. Correlation between $ET_a$ and geographic parameters

For a given region, reference evapotranspiration ( $ET_0$ ) is only determined by weather parameters; however, several factors can affect actual evapotranspiration, such as soil types, current precipitation, crop types, soil moisture storage in the early stage, and field management. We attempted to identify the relationship between  $ET_a$  and geographic parameters

**Table 2** Relationship between  $ET_a$  in summer maize growing season and normalized difference vegetation index (NDVI) and land surface temperature (LST)

Julian day	Relationship between $ET_a$ and NDVI							Relationship between $ET_a$ and LST						
	1	2	3	4	5	6	7	1	2	3	4	5	6	7
2011193	0.22**	-0.04	0.11	-0.09	0.03	0.11	-0.05	-0.42**	-0.48**	-0.15*	-0.49**	-0.44**	-0.31**	-0.33**
2011209	0.32**	0.23**	0.24**	-0.11	0.00	-0.09	0.14	-0.31**	-0.25**	-0.10	-0.21**	-0.23**	-0.32**	-0.22**
2011225	0.14*	0.11	0.13	0.09	-0.08	0.19*	0.03	-0.28**	-0.48**	-0.18*	-0.45**	-0.31**	-0.41**	-0.34**
2011241	0.21**	0.30**	0.10	0.08	0.03	0.07	0.20**	-0.35**	-0.67**	-0.21**	-0.03	-0.19**	-0.17*	-0.28**
2011257	0.30**	0.26**	0.06	0.06	0.17*	0.21**	0.18*	-0.34**	-0.38**	0.16*	-0.47**	-0.28**	-0.08	-0.49**

\* represents linear coefficients significant at  $P < 0.05$ . \*\* represents linear coefficients significant at  $P < 0.01$ . The same as below.

**Table 3** Relationship between  $ET_a$  in winter wheat growing season and NDVI and LST

Julian day	Relationship between $ET_a$ and NDVI							Relationship between $ET_a$ and LST						
	1	2	3	4	5	6	7	1	2	3	4	5	6	7
2011289	0.01	0.12	-0.28**	0.02	-0.11	-0.14*	0.16*	-0.26**	-0.01	0.27**	-0.15*	0.06	-0.12	-0.26**
2011305	0.18*	0.17*	0.29**	0.12	-0.17*	-0.14*	-0.17*	-0.28**	-0.19**	-0.33**	-0.19**	-0.28**	-0.19**	-0.03
2011321	0.17*	0.06	0.35**	0.12	-0.04	-0.08	-0.01	-0.03	0.12	0.42**	0.14*	-0.45**	0.02	0.02
2011337	0.17*	0.11	0.43**	0.11	-0.08	-0.04	0.03	-0.38**	-0.25**	-0.70**	-0.30**	-0.36**	-0.07	0.05
2011353	0.19**	0.16*	0.44**	0.16*	-0.09	-0.01	0.05	-0.19**	0.20**	-0.24**	0.00	-0.42**	-0.16*	-0.45**
2012001	0.18*	0.15*	0.44**	0.16*	-0.07	-0.03	0.04	-0.24**	0.04	-0.36**	-0.16*	-0.45**	-0.40**	-0.30**
2012017	0.18	0.21	0.48	0.15	-0.12	0.06	0.07	-0.32**	-0.12	-0.22**	-0.17*	0.02	-0.19**	-0.10
2012033	0.15*	0.26**	0.56**	0.29**	-0.07	-0.06	0.19*	-0.45**	-0.02	0.09	-0.13	-0.29**	-0.27**	-0.05
2012049	0.18*	0.28**	0.54**	0.29**	-0.17*	-0.02	0.15*	-0.56**	-0.10	-0.15*	-0.48**	-0.15*	-0.22**	-0.15*
2012065	0.15	0.43**	0.55**	0.24**	-0.09	-0.02	0.32**	-0.52**	-0.38**	-0.35**	-0.45**	-0.13	-0.06	-0.29**
2012081	0.22**	0.36**	0.65**	0.19**	-0.05	0.02	0.09	-0.44**	-0.47**	-0.65**	-0.47**	-0.16*	-0.09	-0.26**
2012097	0.17	0.27**	0.67**	0.20**	0.07	-0.05	0.14*	-0.56**	-0.43**	-0.73**	-0.49**	0.05	-0.05	-0.36**
2012113	0.16	0.41**	0.66**	0.16	0.08	-0.03	0.11	-0.06	0.18*	-0.12	-0.32**	-0.27**	-0.18*	-0.28**
2012129	0.21	0.40**	0.57**	0.19**	0.14*	-0.13	0.12	-0.35**	-0.51**	-0.63**	-0.14	-0.30**	-0.47**	-0.50**
2012145	0.25**	0.31**	0.55**	0.14	0.32**	0.05	0.20*	-0.48**	-0.30**	-0.58**	-0.16*	-0.28**	-0.38**	-0.14*
2012161	0.23**	0.26**	0.03	0.21**	0.10	0.12	0.20**	-0.45**	-0.10	0.00	-0.14*	-0.07	-0.19**	0.06

in this study because they may reflect climate fluctuations, changes on soil characteristics, field management and irrigation schemes with geography transitions.  $ET_a$  in the summer maize period represented a significant relationship with longitude ( $P < 0.01$ ), which described an increasing trend from the eastern portion to the western part of 3H Plain (Fig. 3-A). This spatial pattern of  $ET_a$  in the summer maize growing season is in accordance with that of precipitation. Usually, the growing season for summer maize in 3H Plain is from July to September, when there is concentrated precipitation and higher temperature. During this period, less than 20% of  $ET_a$  is from irrigation. When compared to temperature, crop physiology is more sensitive to water for summer maize owing to the sufficient heat resources in the summer maize growing season. Rainfall was considered as the main crop water resource in the eastern part of 3H Plain, where more precipitation was detected in the past 40 years. Supplementary irrigation has always been used in the western part of the region, which is characterized by piedmont plain-irrigable land, low plain-hydroponia irrigable land and dry land.

As shown in Fig. 3-B, the  $ET_a$  for winter wheat had a significant relationship with latitude (with  $R^2 = 0.23$ ,  $P < 0.01$ ), increasing as latitude increased. Winter wheat accounts for about 70% of the total agricultural water use in this area, and precipitation during the winter wheat growing season ranges from 100 to 180 mm (Li *et al.* 2010), which can only meet around 25–40% of the water requirements for the season. Although it is an important area for winter wheat production, rainfall in the region is erratic and limited during the growing stage; accordingly, supplementary irrigation has been widely adopted to ensure maximum production (Sun *et al.* 2006; Li *et al.* 2008). For irrigated wheat, seasonal  $ET_a$  mostly ranges from 400 to 600 mm, 70% of which is derived from irrigation. Spatial differences have not only been found in precipitation, but also in irrigation practices. According to Yang *et al.* (2013), precipitation in the southeast part of 3H Plain can account

for over 50% of the total water consumption for winter wheat. However, irrigation was identified as the dominant water resource in the northern part of 3H Plain, including piedmont plain-irrigable land (Zone 2) and low plain-hydroponia irrigable land and dry land (Zone 3), where irrigation accounts for more than 60% of the winter wheat water consumption.

### 3. Discussion

#### 3.1. Assessment of regional crop evapotranspiration

The findings presented in this paper are the first region-wide, integrated remote sensing, SEBAL model, and ground truth and phenological data to estimate  $ET_a$  in 3H Plain. There are various ways to estimate crop water consumption, most of which are relatively precise at very small scales, but impractical over large scales. Crop water consumption as the main water output in agricultural hydrological processes is necessary to identify experimental field points not only in a controlled environment, but also at regional scales. At regional scales, crop evapotranspiration is often more relevant to policy, agricultural input, soil types and available resources. However, water consumption by crops cannot be accurately identified without crop distribution information (Cai and Sharma 2010). This study is the first attempt to apply regional evapotranspiration model and crop information for assessment of crop (winter wheat and summer maize cropping system) evapotranspiration at a large regional scale, such as 3H Plain. This addition marks the improvement of this research work over numerous previous studies (Zwart and Bastiaanssen 2007; Immerzeel *et al.* 2008; Cai and Sharma 2010; Zwart *et al.* 2010).

#### 3.2. Separation of evapotranspiration of the two crops

A method was developed to extend daily evapotranspiration

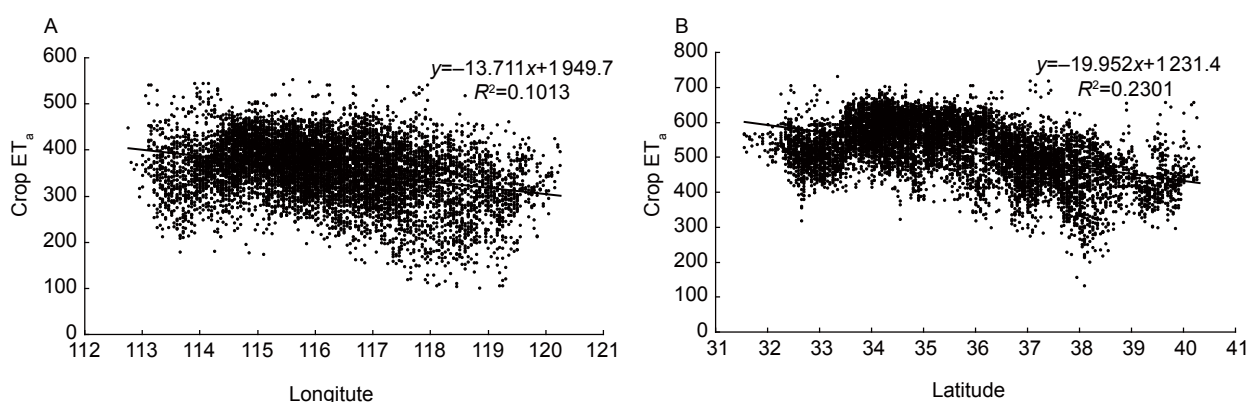


**Fig. 3** Correlation analysis of crop  $ET_a$  and geographic parameters. A, correlation of  $ET_a$  in the summer maize growing season and longitude. B, correlation of  $ET_a$  in the winter wheat growing season and latitude.

to the crop growing season in this study. The extrapolation of daily evapotranspiration to crop growing seasons in pixel level was conducted through spatial interpolation methods based on crop phenological data. Crop (winter wheat and summer maize) phenology data for the 3H Plain, as well as other essential information, was used to obtain pixel crop phenology data. Crop growth is more closely related to latitude and longitude, elevation, crop varieties and meteorological factors, such as air temperature, light and water (Yang *et al.* 2011). However, the method explained in this paper avoided complex factors and parameters above, and can be easily applied elsewhere. Additionally, evapotranspiration extracted from winter wheat and summer maize can be more accurately estimated than the aforementioned factors.

### 3.3. Possible uncertainty of results

The  $ET_a$  in this study was 354.8 and 521.5 mm for summer maize and winter wheat, respectively, which is higher than previous studies (Xiao *et al.* 2009; Chen *et al.* 2012). It is not surprising that  $ET_a$  was lower at the research stations since they are operated under a controlled environment to achieve the maximum water use efficiency, and are less constrained than farmers with regards to resources availability (Yan and Wu 2014). In general, the  $ET_a$  of winter wheat was higher than that of summer maize in 3H Plain. These findings partially agreed with those of Ren and Luo (2004) and Chen *et al.* (2012) who pointed out that crop physiological characteristics, field management measures and irrigation programs are major factors influencing  $ET_a$ , even if reference evapotranspiration ( $ET_0$ ) and crop water requirement ( $ET_c$ ) occasionally showed different characteristics. However, spatial differences have made it possible for a target region to have contrary results. For example, in Hebei Province the  $ET_a$  of summer maize was a slightly higher than that during the winter wheat growing season. Spatial analysis demonstrated a linear relationship between crop  $ET_a$  and NDVI and land surface temperature, which is consistent with the result of a study conducted by Wang (2012). It should be noted that the raster pixel was upscaled to 1 000 m×1 000 m for easier presentation, which may have caused the pixels to merge together, and decreased the relevance between dependent and independent variables. As a result, the correlation coefficient between crop  $ET_a$  and NDVI and land surface temperature may actually be higher than the calculated value.

### 3.4. Need for refinement

It is important to note that there are some uncertainties associated with estimating crop evapotranspiration using remote sensing data and the SEBAL model over a large-scale

region such as 3H Plain. Gathering remote sensing data is a complicated process that must be followed by sensor calibration and atmospheric correction (Cai and Sharma 2010). The spatial distribution of evapotranspiration modeling from SEBAL is 1 000 m×1 000 m; however, mixed cropping patterns and fragmented farming are found common in crop planting extraction research, so sub-pixel area fraction estimation is well accepted (Thenkabail *et al.* 2007a; Hao *et al.* 2011). In some situations, one pixel contains several tapes except target crop, such as water body, residential areas, and forest land. Under the given conditions, the image element may be exaggerated or ignored, which can lead poor estimations and increased errors.

## 4. Conclusion

In this study, actual evapotranspiration for winter wheat and summer maize respectively and its spatial patterns were quantified in 3H Plain. The seasonal average  $ET_a$  of summer maize and winter wheat were 354.8 and 521.5 mm in 3H Plain. A high- $ET$  belt of summer maize covers the piedmont plain, and low  $ET_a$  areas of summer maize are mainly found in the hill-irrigable land and dry land area. For winter wheat, higher  $ET_a$  areas were located in the middle part of 3H Plain, including low plain-hydropenia irrigable land and dry land (Zone 3), hill-irrigable land and dry land (Zone 4), and basin-irrigable land and dry land (Zone 5). Spatial analysis demonstrated a linear relationship between crop  $ET_a$  and NDVI, as well as between  $ET_a$  and land surface temperature. During the crop growing season,  $ET_a$  was more closely related to NDVI in the metaphase and last phase.

We attempted to identify relationships between  $ET_a$  and crop growing season land surface parameters and geographic parameters. NDVI in the metaphase and last phase showed a closer correlation to  $ET_a$  in the crop growing season, and a significant relationship between  $ET_a$  and LST was observed throughout the crop growing season.  $ET_a$  in the summer maize growing season was correlated with longitude, while  $ET_a$  in the winter wheat growing season showed a significant relationship with latitude. Field management (supplemental irrigation) also showed a strong response to the  $ET_a$  pattern in 3H Plain.

## 5. Materials and methods

### 5.1. Study area

Huang-Huai-Hai (3H) Plain in northern China is recognized as one of the largest plains in the country, extending from 31°14' to 40°25' N and 112°33' to 120°17' E (Fig. 4), over an area of about 350 000 km<sup>2</sup>. The climate is characterized by a temperate, sub-humid, and continental monsoon with

an average annual precipitation of 500 to 800 mm (Ren *et al.* 2008). Winter is characterized by insufficient water for winter wheat development and production (Nguyen *et al.* 2011). Nevertheless, 3H Plain is well accepted to be a major agricultural center, accounting for around 61 and 31% of China's wheat and maize production, respectively (Wang *et al.* 2009; Ma *et al.* 2013). Accordingly, the cropping system in the plain is well-known to be a winter wheat-summer maize rotation system (Zhao *et al.* 2006; Liang *et al.* 2011; Sun *et al.* 2011). Currently, it is widely recognized that winter wheat is sown in early October and harvested in June of the second year, and that summer maize is then sown immediately afterwards and harvested in later September. 3H Plain (Fig. 4) is divided into six agricultural sub-regions, coastal land, a farming-fishing area (including the northern part, Zone 1, and the southern part, Zone 7), piedmont plain-irrigable land (Zone 2), low plain-hydroponia irrigable land and dry land (Zone 3), hill-irrigable land and dry land (Zone 4), basin-irrigable land and dry land (Zone 5) and hill-wet hot paddy-paddy field (Zone 6).

## 5.2. Crop dominance map

Ground truth missions were carried out in 3H Plain in October 2011 and May 2012. The missions collected 175

samples from throughout the plain (Fig. 5-A). Detailed crop patterns were recorded including a crop mixture percentage visual estimate, crop growth period and past crop types (Cai and Sharma 2010). The spectral signature curve of the summer maize-winter wheat rotation was extracted based on the sample points (Fig. 5-B). ISODATA (iterative self-organizing data analysis technique) class identification technique and spectral matching technique (SMT) as proposed by Thenkabail *et al.* (2007b), were conducted to improve the summer maize-winter wheat rotation dominance map (Fig. 5-C) using ground truth information as the input. The cultivated area data of 347 counties were used for validation, and the *R* square value was 0.719, suggesting that the generated summer maize-winter wheat rotation dominance map was reliable (Fig. 5-D).

## 5.3. Phenological data

The phenological data for the six agricultural sub-regions of 3H Plain from 2011 to 2012 were acquired from the China Meteorological Administration (CMA). The data included the date of sowing and maturity of winter wheat and summer maize provided by the 50 agricultural meteorological stations in 3H Plain. The average phenology date was calculated for the six agricultural sub-regions. Summer maize was

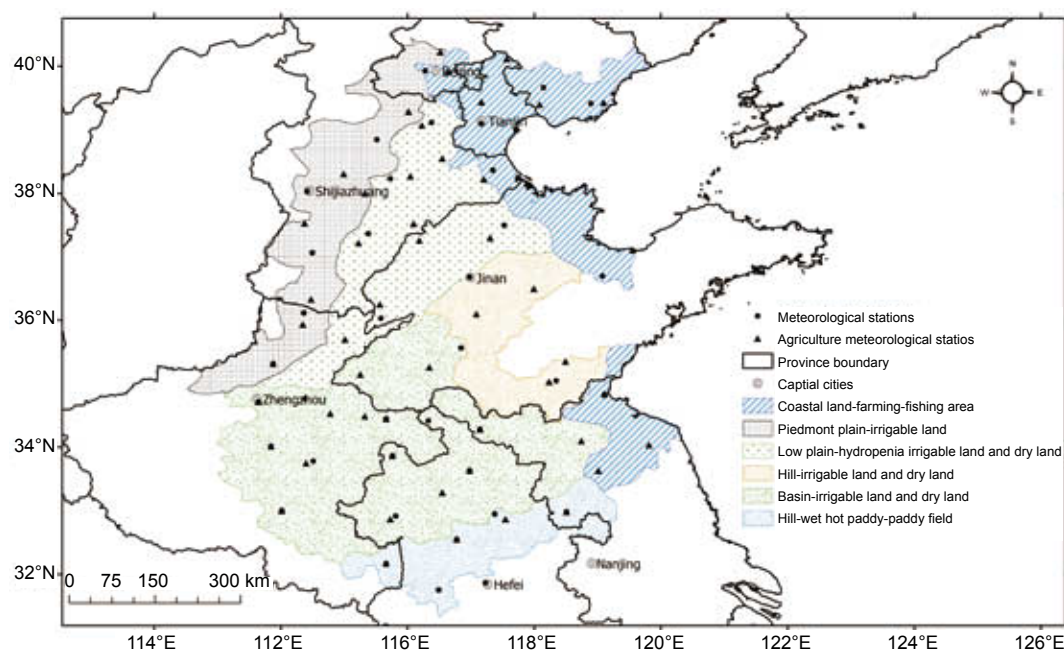


**Fig. 4** The inset map shows the location of Huang-Huai-Hai (3H) Plain and its six agricultural sub regions. The sub regions of 3H Plain include a coastal land-farming-fishing area (including the northern part: Zone 1 and southern part: Zone 7), piedmont plain-irrigable land (Zone 2), low plain-hydroponia irrigable land and dry land (Zone 3), hill-irrigable land and dry land (Zone 4), basin-irrigable land and dry land (Zone 5) and hill-wet hot paddy-paddy field (Zone 6). The locations of the meteorological sites and agricultural meteorological stations are indicated by circles and triangles, respectively.

sown from June 5 to June 20. Summer maize maturity was detected from the middle ten days to the last ten days of September. Winter wheat was sown during October, and harvested during the first ten days of June. Details regarding the phenology date of six agricultural zones are presented in Table 4.

**5.4. MODIS products**

MODIS (moderate-resolution imaging spectroradiometer)

products including MOD11A1 (land surface temperature/surface emissivity), MOD13A2 (NDVI) and MCD43B3 (surface albedo) were downloaded through NASA WIST for use in this study. The spatial accuracy of the three MODIS products is 1 km. The temporal accuracy of MOD11A1, MOD13A2 and MCD43B3 was 1, 16, and 8 d, respectively. For land surface temperature images, cloudy areas were eliminated by replacing the values with the average of two images in the nearest clear dates (Cai and Sharma 2010).

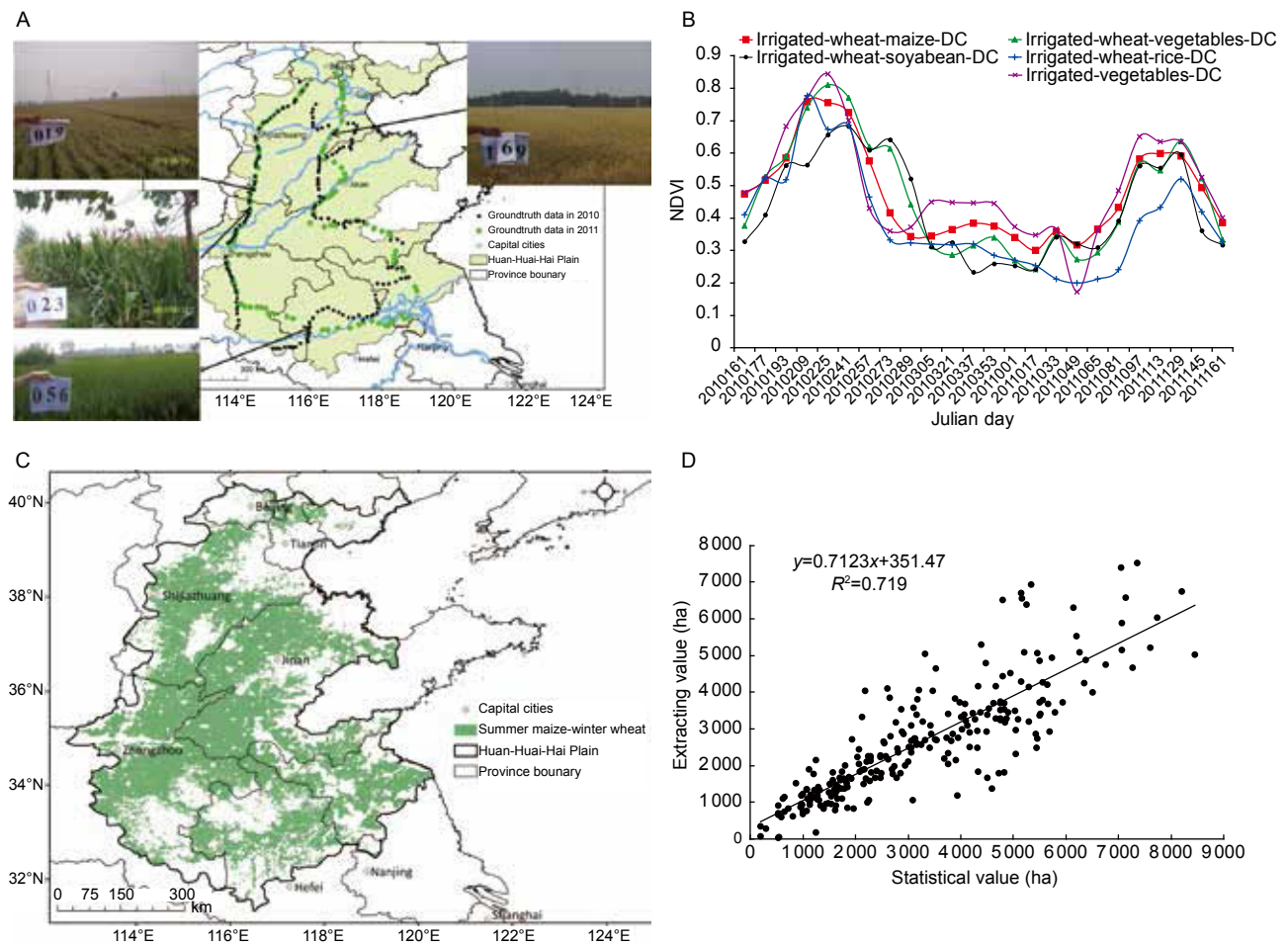


**Fig. 5** Crop dominance map extraction. A, samples distribution in 3H Plain. B, spectral signature of summer maize-winter wheat rotation. C, crop dominance map. D, accuracy analysis.

**Table 4** Average phenology of six sub regions in 3H Plain

Agricultural zoning	Zone number	Summer maize		Winter wheat	
		Sowing	Maturity	Sowing	Maturity
Coastal land-farming-fishing area (north)	Zone 1	6.15	9.25	10.10	6.15
Coastal land-farming-fishing area (south)	Zone 7	6.20	9.20	10.18	6.50
Piedmont plain-irrigable land	Zone 2	6.10	9.22	10.70	6.70
Low plain-hydroponia irrigable land and dry land	Zone 3	6.11	9.24	10.10	6.70
Hill-irrigable land and dry land	Zone 4	6.18	9.24	10.70	6.80
Basin-irrigable land and dry land	Zone 5	6.10	9.20	10.16	6.30
Hill-wet hot paddy-paddy field	Zone 6	6.50	9.16	10.27	5.25

### 5.5. Meteorological data

Meteorological data are also needed for assessment of evapotranspiration. Datasets from 2011 to 2012 from 40 weather stations provided by the China Meteorological Administration (CMA) were used in this study (Fig. 4). The obtained data consisted of the daily observed maximum and minimum air temperature and wind speed measured at 10 m. Wind speed at 2 m was calculated from the wind speed at 10 m according to Allen *et al.* (2007) and interpolated with air temperature over 3H Plain in pixels of 1 000 m, which are needed for inputs in SEBAL.

### 5.6. SEBAL model

**SEBAL model introduction** In this research, the SEBAL model based on remote sensing technology was applied to estimate the daily evapotranspiration (ET). The MODIS data were used to estimate the regional ET for the study area. The calculation of the main parameters by the SABEL model is described below (Cai and Sharma 2010).

The SEBAL model is based on the energy balance equation described by the following equation:

$$R_n = G + H + \lambda ET \tag{1}$$

Where,  $R_n$  ( $W\ m^{-2}$ ) is the net radiation,  $G$  ( $W\ m^{-2}$ ) is the soil heat flux,  $H$  ( $W\ m^{-2}$ ) is the sensible heat flux, and  $\lambda ET$  ( $W\ m^{-2}$ ) is the latent heat flux associated with evapotranspiration.

The net radiation flux on the land surface,  $R_n$  ( $W\ m^{-2}$ ), was calculated using the following equation:

$$R_n = (1 - \alpha)K_{in} + (L_{in} - L_{out}) - (1 - \epsilon)L_{in} \tag{2}$$

Where,  $\alpha$  is the surface albedo,  $K_{in}$  is the incoming short wave radiation ( $W\ m^{-2}$ ),  $L_{in}$  is the incoming long wave radiation ( $W\ m^{-2}$ ),  $L_{out}$  is the outgoing long wave radiation ( $W\ m^{-2}$ ), and  $\epsilon$  is the land surface emissivity.

The soil heat flux is known to primarily depend on land surface characteristics and soil water content. The soil heat flux was calculated for the SEBAL model by the following equation:

$$G = \frac{T - 273.16}{\alpha} \left[ (0.0032 \times \frac{\alpha}{0.9} + 0.0062 \times (\frac{\alpha}{0.9})^2) (1 - 0.98 NDVI^4) R_n \right] \tag{3}$$

The sensible heat flux was calculated using the following equation:

$$H = \frac{\rho_{air} C_p dT}{r_{ah}} \tag{4}$$

Where,  $H$  is the sensible heat flux ( $W\ m^{-2}$ ),  $\rho_{air}$  is the air density ( $kg\ m^{-3}$ ), and  $C_p$  is the air specific heat at constant pressure ( $J\ kg^{-1}\ K^{-1}$ ).

Since the evaporative fraction  $\Lambda$  is constant during a day, the daily  $ET_{24}$  (mm) can be estimated using the following equations:

$$\Lambda = \frac{\lambda ET}{R_n - G} \tag{5}$$

$$ET_{24} = \frac{\Lambda (R_{24} - G_{24})}{\lambda} \tag{6}$$

Where,  $ET_{24}$  is the daily net radiation ( $W\ m^{-2}$ ),  $G_{24}$  is the daily soil heat flux ( $W\ m^{-2}$ ), and  $\lambda$  is the latent heat of vaporization ( $MJ\ kg^{-1}$ ). The SEBAL model is described in detail by Bastiaanssen *et al.* (1998).

**Model validation** In this study, it was difficult to validate the  $ET_a$  map because of its high variability and the low resolution produced by MODIS 1 km products. In recent years, the SEBAL model has been applied and validated in the Americas (Morse *et al.* 2000; Allen *et al.* 2002; Trezza 2002), Europe (Jacob *et al.* 2002; Lagouarde *et al.* 2002), Africa (Bastiaanssen and Menenti 1990; Farah and Bastiaanssen 2001), and China (Li *et al.* 2008). Morse *et al.* (2000) reported that the error in daily ET was 15%, while that in monthly and quarterly ET estimation by SEBAL was 4% in Bear River Basin of Idaho. It was also reported that the error in the estimated daily ET was less than 7% in the Haihe basin (Xiong *et al.* 2006) and less than 8% in the middle region of Heihe basin (Wang *et al.* 2003). Taken together, these studies show that the SEBAL model has good efficiency and applicability for  $ET_a$  estimation. The model also works particularly well in the vegetative area including areas used for maize and wheat agriculture, which was the focus of the present study (Cai and Sharma 2010). Latent heat flux was extracted from the Yucheng station point, and Fig. 6 shows the validation results with the field data for Yucheng station in Shandong Province. The correlation coefficient between the estimated and measured values was 0.888, with a  $P < 0.01$ . Additionally, Table 5 compares the ranges of  $ET_a$  values from this study with those of previous studies. Taken together, these results show that SEBAL is suitable for estimating evapotranspiration in winter wheat

**Table 5** Comparison of  $ET_a$  of maize and wheat growing season for 3H plain from this study and previously reported values

Loctions	Crop	$ET_a$ (mm)		References
		This study	Literature	
Yucheng, Shandong	Wheat	456	(400–500) 450	Chen <i>et al.</i> (2012)
Yucheng, Shandong	Maize	349	(300–370) 350	Chen <i>et al.</i> (2012)
Xinxiang, Henan	Wheat	521	(374.9–551.7)	Xiao <i>et al.</i> (2009)
Piedmont plain	Wheat	400–550	460	Ren and Luo (2004)
Piedmont plain	Maize	300–500	390	Ren and Luo (2004)

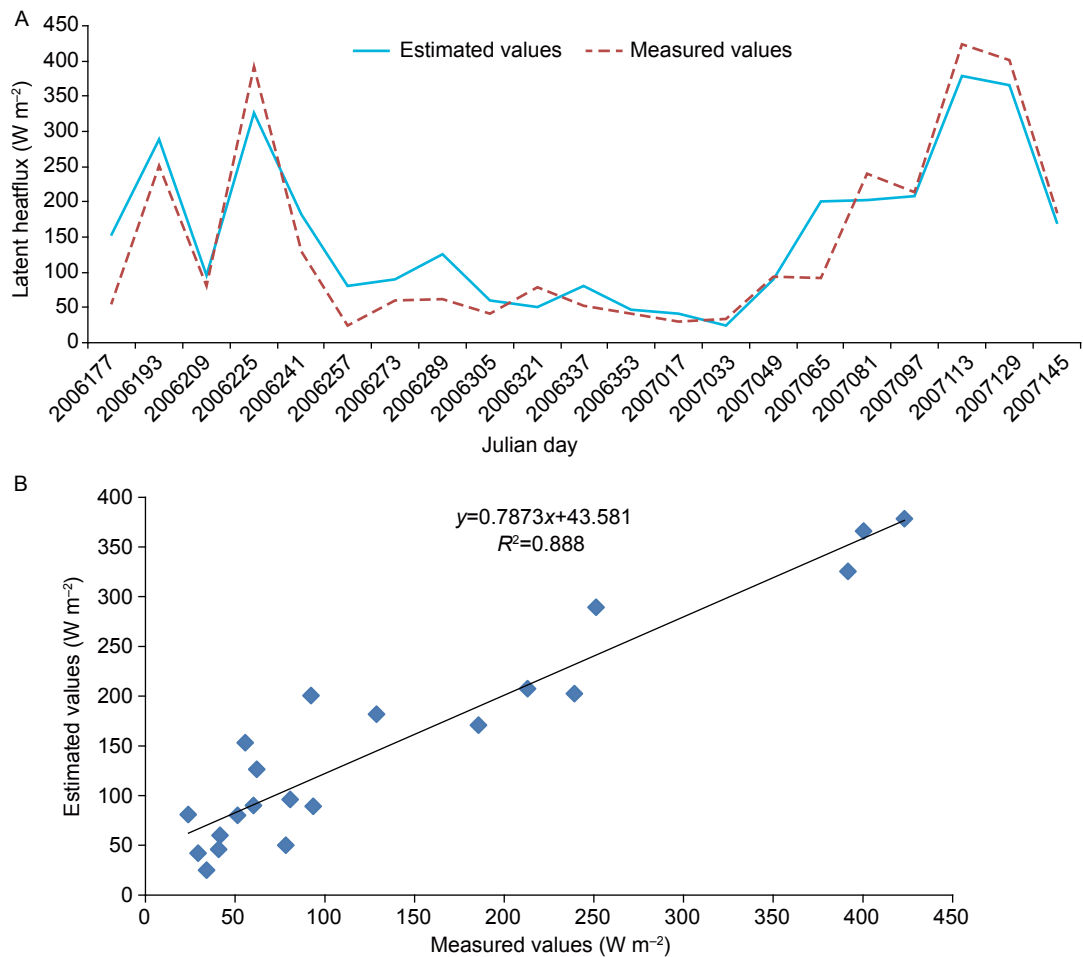


**Fig. 6** Validation results based on field data from Yucheng station. A, comparison of estimated and measured values. B, scatter plot of estimated and measured values.

and summer maize rotation in 3H Plain.

## Acknowledgements

This research was supported by the National Key Technologies R&D Program of China during the 12th Five-Year Plan period (2012BAD09B01), the National Basic Research Program of China (973 Program, 2012CB955904) and the National Science Foundation for Young Scientists of China (41401510). We gratefully acknowledge Prof. Vinay Nangia, agricultural hydrologist, from the International Center for Agricultural Research in the Dry Areas (ICARDA) for his English editing and the University of Liège-Gembloux Agro-Bio Tech and more specifically the research platform AgricultureLife.be for the funding a scientific stay in Belgium in the framework of this research project.

## References

- Ali M H, Talukder M. 2008. Increasing water productivity in crop production—a synthesis. *Agricultural Water Management*, **95**, 1201–1213.
- Allen R G, Morse A, Tasumi M, Trezza R, Bastiaanssen W, Wright J L, Kramber W. 2002. Evapotranspiration from a satellite-based surface energy balance for the Snake Plain Aquifer in Idaho. In: *Proceedings of the USCID/EWRI Conference on Energy, Climate, Environment and Water Issues and Opportunities for Irrigation and Drainage*. San Luis Obispo, California, USA. pp. 167–178.
- Allen R G, Tasumi M, Trezza R. 2007. Satellite-based energy balance for mapping evapotranspiration with internalized calibration (METRIC)—Model. *Journal of Irrigation and Drainage Engineering*, **133**, 380–394.
- Bastiaanssen W, Menenti M. 1990. Mapping groundwater losses in the western desert of Egypt with satellite measurements of surface reflectance and surface temperature. *Proceedings and Information-TNO Committee on Hydrological Research*, **42**, 61–90.
- Bastiaanssen W, Menenti M, Feddes R A, Holtslag A. 1998. A remote sensing surface energy balance algorithm for land (SEBAL). 1. Formulation. *Journal of Hydrology*, **212**,

- 198–212.
- Brewster M, Herrmann T, Bleish B, Pearl R. 2006. *A Gender Perspective on Water Resources and Sanitation*. Spring, Wagadu. pp. 1–23.
- Cai X L, Sharma B R. 2010. Integrating remote sensing, census and weather data for an assessment of rice yield, water consumption and water productivity in the Indo-Gangetic river basin. *Agricultural Water Management*, **97**, 309–316.
- Carruthers I, Rosegrant M W, Seckler D. 1997. Irrigation and food security in the 21st century. *Irrigation and Drainage Systems*, **11**, 83–101.
- Chen B, Ou Y, Chen W, Liu L. 2012. Water consumption for winter wheat and summer maize in the North China Plain in recent 50 years. *Journal of Natural Resources*, **27**, 1186–1199. (in Chinese).
- Chen J, Tang C, Sakura Y, Yu J, Fukushima Y. 2005. Nitrate pollution from agriculture in different hydrogeological zones of the regional groundwater flow system in the North China Plain. *Hydrogeology Journal*, **13**, 481–492.
- Chen S, Zhang X, Liu M. 2002. Soil temperature and soil water dynamics in wheat field mulched with maize straw. *Chinese Journal of Agrometeorology*, **23**, 34–37. (in Chinese)
- Courault D, Seguin B, Olioso A. 2005. Review on estimation of evapotranspiration from remote sensing data: From empirical to numerical modeling approaches. *Irrigation and Drainage Systems*, **19**, 223–249.
- FAO (Food and Agriculture Organization). 1994. The state of food and agriculture 1993. Food and Agriculture Organization. Rome, Italy.
- Farah H O, Bastiaanssen W. 2001. Spatial variations of surface parameters and related evaporation in the Lake Naivasha Basin estimated from remote sensing measurements. *Hydrological Processes*, **15**, 1585–1607.
- Hao W P, Mei X R, Cai X L, Du J T, Liu Q. 2011. Crop planting extraction based on multi-temporal remote sensing data in Northeast China. *Transactions of the CSAE*, **27**, 201–207. (in Chinese).
- Immerzeel W W, Gaur A, Zwart S J. 2008. Integrating remote sensing and a process-based hydrological model to evaluate water use and productivity in a south Indian catchment. *Agricultural Water Management*, **95**, 11–24.
- Jacob F, Olioso A, Gu X F, Su Z, Seguin B. 2002. Mapping surface fluxes using airborne visible, near infrared, thermal infrared remote sensing data and a spatialized surface energy balance model. *Agronomie*, **22**, 669–680.
- Jia J, Liu C. 2002. Groundwater dynamic drift and response to different exploitation in the North China Plain: A case study of Luancheng County, Hebei Province. *Acta Geographica Sinica*, **57**, 201–209. (in Chinese)
- Jia Z, Liu S, Xu Z, Chen Y, Zhu M. 2012. Validation of remotely sensed evapotranspiration over the Hai River Basin, China. *Journal of Geophysical Research (Atmospheres)*, **17**, D13.
- Jiang J, Zhang Y. 2004. Soil-water balance and water use efficiency on irrigated farmland in the North China Plain. *Journal of Soil and Water Conservation*, **18**, 61–65. (in Chinese)
- Lagouarde J, Jacob F, Gu X F, Olioso A, Bonnefond J, Kerr Y, Mcaneny K J, Irvine M. 2002. Spatialization of sensible heat flux over a heterogeneous landscape. *Agronomie-Sciences des Productions Vegetales Environnement*, **22**, 627–634.
- Li H, Zheng L, Lei Y, Li C, Liu Z, Zhang S. 2008. Estimation of water consumption and crop water productivity of winter wheat in North China Plain using remote sensing technology. *Agricultural Water Management*, **95**, 1271–1278.
- Li Q, Dong B, Qiao Y, Liu M, Zhang J. 2010. Root growth, available soil water, and water-use efficiency of winter wheat under different irrigation regimes applied at different growth stages in North China. *Agricultural Water Management*, **97**, 1676–1682.
- Liang W, Carberry P, Wang G, L R, L H, Xia A. 2011. Quantifying the yield gap in wheat-maize cropping systems of the Hebei Plain, China. *Field Crops Research*, **124**, 180–185.
- Liu S, Mo X, Lin Z, Xu Y, Ji J, Wen G, Richey J. 2010. Crop yield responses to climate change in the Huang-Huai-Hai Plain of China. *Agricultural Water Management*, **97**, 1195–1209.
- Ma Y, Feng S Y, Song X F. 2013. A root zone model for estimating soil water balance and crop yield response to deficit irrigation in the Northern China Plain. *Agricultural Water Management*, **127**, 13–24.
- Molden D, Murray-Rust H, Sakthivadivel R, Makin I. 2003. A water-productivity framework for understanding and action. In: *Water Productivity in Agriculture: Limits and Opportunities for Improvement*. CABI Publishing, Wallingford, UK. pp. 1–18.
- Morse A, Tasumi M, Allen R G, Kramber W J. 2000. *Application of The SEBAL Methodology for Estimating Consumptive Use of Water and Streamflow Depletion in the Bear River Basin of Idaho Through Remote Sensing*. Idaho Department of Water Resources—University of Idaho, USA.
- Nguyen T T, Qiu J J, Ann V, Li H, Eric V R. 2011. Temperature and precipitation suitability evaluation for winter wheat and summer maize cropping system in the Huang-Huai-Hai Plain of China. *Agricultural Sciences in China*, **10**, 275–288.
- De Oliveira A S, Trezza R, Holzapfel E A, Lorite I, Paz V P S. 2009. Irrigation water management in Latin America. *Chilean Journal of Agricultural Research*, **69**, 7–16.
- Perry C. 2011. Accounting for water use: Terminology and implications for saving water and increasing production. *Agricultural Water Management*, **98**, 1840–1846.
- Ren H, Luo Y. 2004. The experimental research on the water-consumption of winter wheat and summer maize in the Northwest plain of Shandong Province. *Journal of Irrigation and Drainage*, **23**, 37–39. (in Chinese)
- Ren J, Chen Z, Zhou Q, Tang H. 2008. Regional yield estimation for winter wheat with MODIS-NDVI data in Shandong, China. *International Journal of Applied Earth Observation and Geoinformation*, **10**, 403–413.
- Rosegrant M W, Cai X M, Cline S A, Cai X. 2002. Global water outlook to 2025: Averting an impending crisis. In: *IFPRI-2020 Vision/International Water Management Institute, Internat. Food Policy Institute, Washington, D.C.* p. 26.

- Rwasoka D T, Gumindoga W, Gwenzi J. 2011. Estimation of actual evapotranspiration using the Surface Energy Balance System (SEBS) algorithm in the Upper Manyame catchment in Zimbabwe. *Physics and Chemistry of the Earth (Parts A/B/C)*, **36**, 736–746.
- Sun H, Liu C, Zhang X, Shen Y, Zhang Y. 2006. Effects of irrigation on water balance, yield and WUE of winter wheat in the North China Plain. *Agricultural Water Management*, **85**, 211–218.
- Sun H, Zhang Y, Zhang X, Mao X, Pei D, Gao L. 2003. Effects of water stress on growth and development of winter wheat in the North China Plain. *Acta Agriculturae Boreali-Sinica*, **18**, 23–26. (in Chinese)
- Sun Q, Krbel R, Mller T, Rmhheld V, Cui Z, Zhang F, Chen X. 2011. Optimization of yield and water-use of different cropping systems for sustainable groundwater use in North China Plain. *Agricultural Water Management*, **98**, 808–814.
- Teixeira A D C, Bassoi L H. 2009. Crop water productivity in semi-arid regions: From field to large scales. *Annals of Arid Zone*, **48**, 1–13.
- Teixeira A D C, Bastiaanssen W, Ahmad M D, Bos M G. 2009. Reviewing SEBAL input parameters for assessing evapotranspiration and water productivity for the Low-Middle Sao Francisco River basin, Brazil: Part A: Calibration and validation. *Agricultural and Forest Meteorology*, **149**, 462–476.
- Thenkabail P S, Biradar C M, Noojipady P, Cai X L, Dheeravath V, Li Y J, Velpuri M, Gumma M K, Pandey S. 2007a. Sub-pixel area calculation methods for estimating irrigated areas. *Sensors*, **7**, 2519–2538.
- Thenkabail P S, GangadharaRao P, Biggs T, Krishna M, Turrall H. 2007b. Spectral matching techniques to determine historical land-use/land-cover (LULC) and irrigated areas using time-series 0.1-degree AVHRR Pathfinder datasets. *Photogrammetric Engineering & Remote Sensing*, **73**, 1029–1040.
- Trezza R. 2002. Evapotranspiration using a satellite-based surface energy balance with standardized ground control. Ph D thesis, Utah State University, Logan, UT, USA.
- Wang E, Chen C, Yu Q. 2009. Modeling the response of wheat and maize productivity to climate variability and irrigation in the North China Plain. In: *18th World IM4CSIMODSIM Congress*. Cairns, Australia. pp. 2742–2748.
- Wang J, Gao F, Liu S. 2003. Remote sensing retrieval of evapotranspiration over the scale of drainage basin. *Remote Sensing Technology and Application*, **18**, 332–338. (in Chinese)
- Wang S, Song X, Wang Q, Xiao G, Liu C, Liu J. 2009. Shallow groundwater dynamics in North China Plain. *Journal of Geographical Sciences*, **19**, 175–188.
- Wang W T, Zhao Q L, Du J. 2012. Advances in the study of evapotranspiration of regional land surface based on remote sensing technology. *Remote Sensing for Land and Resources*, **24**, 1–7. (in Chinese)
- Xiao J, Liu Z, Duan A. 2009. Studies on water production function of winter wheat in Xinxiang district. *Journal of Henan Agricultural University*, **1**, 55–59. (in Chinese)
- Xiong J, Wu B, Zhou Y, Li J. 2006. Estimating evapotranspiration using remote sensing in the Haihe basin. *International Geoscience and Remote Sensing Symposium*. Denver, Colorado, USA. pp. 1044–1047.
- Yan N, Wu B. 2014. Integrated spatial-temporal analysis of crop water productivity of winter wheat in Hai Basin. *Agricultural Water Management*, **133**, 24–33.
- Yang J, Liu Q, Mei X, Yan C, Ju H, Xu J. 2013. Spatiotemporal characteristics of reference evapotranspiration and its sensitivity coefficients to climate factors in Huang-Huai-Hai Plain, China. *Journal of Integrative Agriculture*, **12**, 2280–2291.
- Yang J, Mei X, Liu Q, Yan C, He W, Liu E, Liu S. 2011. Variations of winter wheat growth stages under climate changes in northern China. *Chinese Journal of Plant Ecology*, **35**, 623–631. (in Chinese)
- Yang X L, Gao W S, Shi Q H, Chen F, Chu Q Q. 2013. Impact of climate change on the water requirement of summer maize in the Huang-Huai-Hai farming region. *Agricultural Water Management*, **124**, 20–27.
- Yang Z, Sinclair T R, Zhu M, Messina C D, Cooper M, Hammer G L. 2012. Temperature effect on transpiration response of maize plants to vapour pressure deficit. *Environmental and Experimental Botany*, **78**, 157–162.
- Zhang H, Wang X, You M, Liu C. 1999. Water-yield relations and water-use efficiency of winter wheat in the North China Plain. *Irrigation Science*, **19**, 37–45.
- Zhao R F, Chen X P, Zhang F S, Zhang H, Schroder J, Rmhheld V. 2006. Fertilization and nitrogen balance in a wheat-maize rotation system in North China. *Agronomy Journal*, **98**, 938–945.
- Zwart S J, Bastiaanssen W G. 2007. SEBAL for detecting spatial variation of water productivity and scope for improvement in eight irrigated wheat systems. *Agricultural Water Management*, **89**, 287–296.
- Zwart S J, Bastiaanssen W G, de Fraiture C, Molden D J. 2010. WATPRO: A remote sensing based model for mapping water productivity of wheat. *Agricultural Water Management*, **97**, 1628–1636.

(Managing editor SUN Lu-juan)